

## EXPERIMENTAL STUDY OF VIBRATION CONTROL IN A 3 DOF PITCH-PLANE MODEL OF AN MR VEHICLE SUSPENSION

### SUMMARY

*The paper is concerned with the experimental study of vibration control in a vehicle suspension model equipped with independently controlled magnetorheological (MR) dampers in front and rear sections of the vehicle body, and in the driver's seat suspension. Pitch-plane suspension model with one pitch degree of freedom (DOF) and two bounce DOFs was considered. The system was tested under harmonic excitations with an open loop and feedback. Performance of standard skyhook controller was compared with cascade controllers, in which the reference resistance forces determined by linear-quadratic or skyhook principles were fed to the inverse model of an MR damper. The tests were conducted in the experimental setup with measurement and control system configured in MATLAB/Simulink environment.*

**Keywords:** MR damper, pitch-plane suspension model, vibration control

### STEROWANIE DRGANIAMI PŁASKIEGO MODELU ZAWIESZENIA POJAZDU O TRZECH STOPNIACH SWOBODY – ANALIZA EKSPERYMENTALNA

*W artykule przedstawiono analizę eksperymentalną układu sterowania drganiami modelu zawieszenia pojazdu wyposażonego w niezależnie sterowane tłumiki magnetoreologiczne (MR) umiejscowione w przednim i tylnym zawieszeniu nadwozia pojazdu, oraz w zawieszeniu fotela kierowcy/operatora. Rozważono płaski model zawieszenia posiadający jeden stopień swobody związany z przechyłem wzdłużnym oraz dwa stopnie swobody związane z przemieszczeniem pionowym. Przeprowadzono badania układu otwartego oraz układu zamkniętego przy wymuszeniach harmonicznym. Dokonano porównania działania regulatora typu skyhook z regulatorami kaskadowymi, dla których referencyjne siły oporu uzyskane jako wyjścia algorytmu skyhook lub rozwiązania problemu liniowo-kwadratowego były odwzorowywane z wykorzystaniem modelu odwrotnego tłumika MR. Badania przeprowadzono na stanowisku laboratoryjnym z wykorzystaniem układu pomiarowo-sterującego skonfigurowanego w środowisku MATLAB/Simulink.*

**Słowa kluczowe:** tłumik MR, płaski model zawieszenia, sterowanie drganiami

### 1. INTRODUCTION

The type of the model selected for the purpose of vibration analysis is largely dependent on the objective of the analysis. The suspended body (sprung mass) of a vehicle may possess flexibility, which increases the amplitude of structural vibration modes, characterised by significantly higher frequencies than modes associated with the suspension operation. For the ride vibration analysis, therefore, all wheeled road and off-road vehicles can be described by a 7 DOF suspension model [19], where respective DOFs represent bounce, roll and pitch motions of sprung mass, and bounce motions of the four unsprung masses of wheels assemblies (independent wheel suspensions are considered). At low frequencies the vehicle body, represented by its sprung mass, moves as an integral unit supported on the primary suspension system. Wheels, axles and brake hardware are represented by the unsprung masses in contact with the road surface through the tires. In response to the road roughness, the unsprung masses move as rigid bodies acting on (exciting) the sprung mass. The passengers or goods occupying the sprung mass are directly subjected to vibrations. Thus the motion of the

sprung mass and also unsprung masses is the primary concern of the ground vehicles vibration analysis [1].

Typical vehicle suspensions with passive dampers are characterised by unavoidable compromise between road roughness attenuation and drive stability. That is why active and semi-active vehicle suspensions are used. In semi-active suspensions the conventional springs are retained but passive dampers are replaced by controllable dampers, e.g. with variable orifice [12] or variable viscosity of the filling fluid as for MR dampers [8]. These suspensions systems use external power supply only to adjust the damping levels and operate the controller and sensors.

The review of simple but credible models that can be useful for fundamental vibration analysis in terms of resonant frequencies and forced vibration response of sprung and unsprung masses reveals that the vibration response of vehicles to different excitations can be investigated through the analysis of various in-plane models [11, 12]. Because the wheelbase of the majority of ground vehicles is significantly larger than the track width, the roll motions can be considered negligible compared to the magnitudes of vertical and pitch motions. That is why we focused on a pitch-plane model of the

\* Department of Process Control, AGH University of Science and Technology, Cracow, Poland; deep@agh.edu.pl, pmartyn@agh.edu.pl

vehicle suspension, extended with the driver's seat suspension [10] that could be regarded also as vehicle cab suspension. The model is equipped with MR dampers. We assume negligible contributions due to tires damping, and tires stiffness that is 6–10 times higher than that of primary suspension. It means the road input is taken to be the same as the wheels input. Such a model is considered applicable for study of off-road vehicles without tires (caterpillar vehicles: excavators, tanks, etc.) or without primary suspension – then stiffness and damping factors apply to the tires properties alone.

The model to be investigated comprises two independent spring – MR damper sets within the primary suspension and the third spring – MR damper set that represents the suspension of driver's seat. Such a 3 DOF model enables us to study bounce and pitch motions of the suspended body, bounce of the driver, and to analyse vibration modes assuming negligible contributions due to the unsprung assembly.

## 2. PITCH-PLANE MODEL

The diagram of 3 DOF pitch-plane model is depicted in Figure 1. The suspended body is simulated by a rigid rectangle-intersection beam of mass  $m$ , length  $L$ , height  $a$ , width  $b$ , and centre of gravity (c.o.g.) in  $P_g$ . The beam is supported in points  $P_f$  and  $P_r$  by two identical spring – MR damper sets (hereinafter called suspension-sets), which are subject to base displacement excitations similar to these acting upon conventional vehicle suspension. Distances from  $P_g$  to  $P_f$  and from  $P_g$  to  $P_r$  are denoted by  $l_f$  and  $l_r$ . Elasticity factors of the front and rear springs are denoted by  $k_f$  and  $k_r$ . Similarly,  $i_f$  and  $i_r$  denote currents in the front ( $d_f$ ) and rear ( $d_r$ ) MR dampers' coils,  $F_{df}$  and  $F_{dr}$  – resistance forces produced by  $d_f$  and  $d_r$ . Excitations applied to the base of front and rear suspension-sets are denoted by  $w_f$  and  $w_r$ , displacements of points  $P_f$  and  $P_r$  by  $x_f$  and  $x_r$ . Additionally, the model consists of a rigid plate of mass  $m_s$  (modeling the driver and the seat), suspended in  $P_g$  on spring – MR damper ( $d_s$ ) set. The elasticity factor of the spring is  $k_s$ , current in the MR damper  $d_s$  coil is  $i_s$ , resistance force produced by  $d_s$  is  $F_{ds}$ . This model possesses 3 DOFs: vertical (bounce) displacement  $x$  and pitch displacement  $\varphi$  of the beam, and relative bounce displacement  $x_s$  of rigid plate with respect to and perpendicular to the beam.

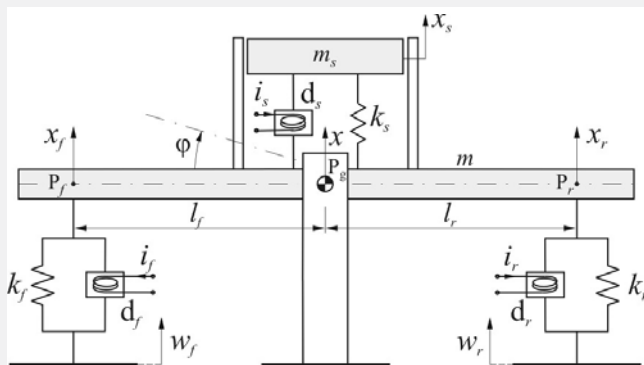


Fig. 1. Diagram of 3 DOF pitch-plane model of MR vehicle suspension

The mechanical constraints of the system motion are ensured with rigid stabilizing vertical guides positioned symmetrically on two sides of the beam (to restrict the motion of the beam's c.o.g.). Values of the model parameters are as follows:  $l_f = 0.7$  m,  $l_r = 0.7$  m,  $L = 1.5$  m,  $a = 0.129$  m,  $b = 0.120$  m,  $m = 191.68$  kg,  $m_s = 66.73$  kg,  $k_f = 42\,016$  N/m,  $k_r = 42\,016$  N/m,  $k_s = 31\,565$  N/m.

## 3. FEEDBACK SYSTEM

As one of the basic suspension purposes is optimisation of drive comfort – minimisation of vibrations affecting humans, mainly within the frequency range of (4, 8) Hz – we implemented a feedback system, whose aim is to reduce root-mean-square (RMS) bounce acceleration transmissibility indexes  $T_{\ddot{x}}$  (2.1),  $T_{\ddot{x}_s}$  (2.2),  $T_C$  (2.3), and frequency weighted RMS ( $f$ -weighted RMS) bounce acceleration transmissibility indexes  $V_{\ddot{x}}$  (2.4),  $V_{\ddot{x}_s}$  (2.5),  $V_C$  (2.6).

$$T_{\ddot{x}} = \frac{RMS(\ddot{x})}{RMS(\ddot{w})} \quad (2.1)$$

$$T_{\ddot{x}_s} = \frac{RMS(\ddot{x} + \ddot{x}_s)}{RMS(\ddot{x})} \quad (2.2)$$

$$T_C = \frac{RMS(\ddot{x} + \ddot{x}_s)}{RMS(\ddot{w})} \quad (2.3)$$

$$V_{\ddot{x}} = \sqrt{\sum_{f \in \Theta} [W(f)T_{\ddot{x}}(f)]^2} \quad (2.4)$$

$$V_{\ddot{x}_s} = \sqrt{\sum_{f \in \Theta} [W(f)T_{\ddot{x}_s}(f)]^2} \quad (2.5)$$

$$V_C = \sqrt{\sum_{f \in \Theta} [W(f)T_C(f)]^2} \quad (2.6)$$

To obtain RMS acceleration transmissibilities:  $T_{\ddot{x}}$ ,  $T_{\ddot{x}_s}$ ,  $T_C$ , system response to the harmonic excitations for the frequencies  $f \in \Theta$  has to be determined ( $\Theta$  is the discrete set of considered excitation frequencies within the range of (2, 10) Hz). Next, the RMS values of absolute accelerations of: beam c.o.g. bounce  $RMS(\ddot{x})$ , seat bounce  $RMS(\ddot{x} + \ddot{x}_s)$  (assuming synchronous excitation type, i.e.  $\varphi = 0$ ), average shakers excitations  $RMS(\ddot{w})$  ( $w = 0.5w_f + 0.5w_r$ ) have to be calculated at each frequency  $f$ . The  $f$ -weighted RMS bounce acceleration transmissibility indexes  $V_{\ddot{x}}$ ,  $V_{\ddot{x}_s}$ ,  $V_C$  will be calculated as recommended in [3] according to the principal weightings  $W(f)$  ( $f \in \Theta$ ). We will also determine bounce displacement amplitude transmissibilities  $T_x = A(x)/A(w)$  and  $T_{x_s} = A(x + x_s)/A(x)$ , where  $A(\bullet)$  states for amplitude.

The control of active and semiactive vehicle suspension systems has been widely investigated. Various control techniques have been used: skyhook control [4, 14], linear-quadratic control [12, 13, 16, 17], sliding mode control [6, 18, 20], fuzzy logic control ([5, 19]), heuristic control [2, 11] and other.

We consider here feedback control strategy described in [8], and also (for 2 DOF model) in [15] – the cascade controller [6, 12, 16, 18, 20] consisting of the two stages:

- 1) Determination of MR dampers' resistance forces reference values (denoted by:  $F_{df}^*$ ,  $F_{dr}^*$ ,  $F_{ds}^*$ ), which minimise the assumed performance index.
- 2) Calculation of the values of currents:  $i_f^*$ ,  $i_r^*$ ,  $i_s^*$ , which cause MR dampers  $d_f$ ,  $d_r$ ,  $d_s$  to produce (for the instantaneous relative velocities: beam–shakers, seat–beam) resistance forces equal to  $F_{df}^*$ ,  $F_{dr}^*$ ,  $F_{ds}^*$  (respectively). This stage utilises the nonlinear inverse model (IM) of an MR damper.

At the first stage of the control task we use linear-quadratic (LQ) algorithm with the integral of beam and seat accelerations over time as a performance index [7] (Fig. 2).

Alternatively, skyhook (SH) principle was used at the first stage of the cascade controller to determine values of  $F_{df}^*$ ,  $F_{dr}^*$ ,  $F_{ds}^*$  (Fig. 3).

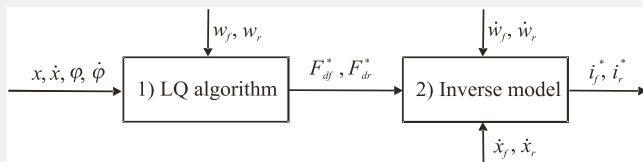


Fig. 2. Diagram of LQ IM controller (linear-quadratic in conjunction with inverse model)

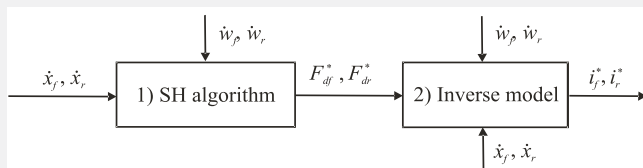


Fig. 3. Diagram of SH IM controller (skyhook in conjunction with inverse model)

The IM (utilised at the second stage of the controller) was obtained on the basis of MR damper resistance force measurements, conducted for the various velocity levels in the range of  $(0, 130) \cdot 10^{-3}$  m/s, and various control currents in the range of  $(0.0, 0.2)$  A.

The values  $F_{df}^*$ ,  $F_{dr}^*$ ,  $F_{ds}^*$  can be produced only for the same signs of velocities:  $\dot{x}_f$  and  $\dot{x}_f - \dot{w}_f$ ,  $\dot{x}_r$  and  $\dot{x}_r - \dot{w}_r$ ,  $\dot{x} + \dot{x}_s$  and  $\dot{x}_s$  (respectively), where:  $x = (x_f + x_r)/2$ . Even then, realisation of forces  $F_{df}^*$ ,  $F_{dr}^*$ ,  $F_{ds}^*$  is not precise due to control circuit time-delays and MR dampers inverse modelling inaccuracy. Above reasons result in quasi-optimal behaviour of such constructed cascade controllers.

The feedback system with standard SH controller was used for vibration isolation performance comparison.

#### 4. EXPERIMENTS

Below we present the mechanical structure of the experimental setup, measurement and control equipment configured in MATLAB/Simulink environment, experimental results and discussion.

##### 4.1. Experimental setup

As our analysis is limited to pitch-plane oscillations, the experimental setup should possess the appropriate transverse rigidity. The other demand states excitations have to be stationary. Limited output of the shakers available in the laboratory conditions and relatively high damping coefficient of the MR dampers we dispose of (RD-1005-3 series by Lord Co.), both imply crucial constraints to the total mass and moment of inertia of the sprung system.

The experimental setup (Fig. 4) consists of steel beam (modelling vehicle body) and steel plate supported in the central part of the beam (modelling the driver and the seat) as load elements, three suspension-sets: spring – MR damper, central stabilizing guiding columns with car elements moving inside them, two kinematic shakers.

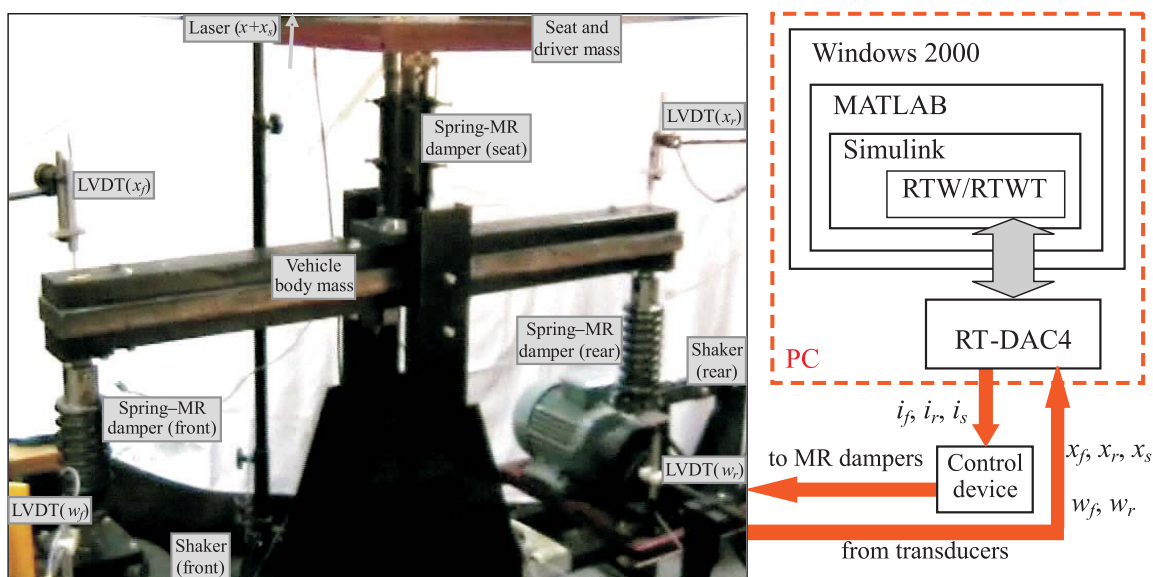


Fig. 4. Experimental setup: mechanical structure, measurement and control equipment

Each of the two beam suspension-sets is built as a parallel connection of a vertically mounted MR damper inside and outer screw-cylindrical reflex spring guided onto two thin-wall sleeves. The sleeves are guided one inside the other with teflon slide ring between them. Each of these suspension-sets is connected at the top with the beam; the base is connected with the respective shaker by means of pin joints. The suspension of the steel plate includes cylindrically mounted MR damper inside and screw-cylindrical reflex spring outside, guided by two outer metal sleeves, moving one inside another. The lower sleeve is mounted rigidly, perpendicularly to the beam, the upper one – to the seat.

Two types of shakers were available in the experiments. One of them (front) is an electro-hydraulic cylinder with maximum force output  $2.5 \cdot 10^3$  N and maximum stroke  $50 \cdot 10^{-3}$  m, the other (rear) is an asynchronous electric motor (nominal power of  $3.5 \cdot 10^3$  W) with controllable circular cam crank mechanism, supplied by the electronic inverter enabling smooth control of rotation speed and excitation frequency within the range of (2.5, 10) Hz. The c.o.g. of the beam is guided and vertically stabilised by means of two car elements located symmetrically on both sides of the beam, moving inside vertical steel guides (bearing systems offering backlash elimination were implemented) [9].

The measurements were conducted by means of four PSz-20 LVDTs (two of them located on the beam –  $x_f$  and  $x_r$ , the other two on the shakers –  $w_f$  and  $w_r$ ), one laser transducer for steel plate absolute displacement (equal to  $x + x_s$  for  $\varphi = 0$ ) measurement, and a multi I/O board of RT-DAC4 series placed in a standard PC (Fig. 4). On the basis of  $x_f$  and  $x_r$  measurement, vertical displacement  $x$  and pitch displacement  $\varphi$  of the beam, and steel plate relative displacement  $x_s$  were obtained. MATLAB/Simulink environment with RTWT (Real-Time Windows Target) extension of RTW (Real-Time Workshop) toolbox running on Windows 2000 operating system was used. The currents  $i_f, i_r, i_s$  calculated in MATLAB/Simulink were output to MR dampers' coils by means of RTWT/RTW, the RT-DAC4 board, and the control device.

The experimental setup configuration – relatively large steel plate mass (tuned for RD-1005-3 parameters) and insufficient transversal rigidity of its suspension – imposed synchronous excitation type only, i.e.  $w_f = w_r$ , thus no pitch of the beam  $\varphi$  should appear. For the asynchronous excitations, the behaviour of the steel plate was altered by the considerable forces acting perpendicularly to the seat suspension guides. The other concern was quality of the excitation signal  $w_r$ , which revealed the circular cam crank shaker inaccuracy, mainly at low frequencies (below 4 Hz).

To produce the synchronous excitation, the semi-sine excitation  $w_r$  was duplicated by the electro-hydraulic shaker ( $w_f$ ). The actual value of  $w_r$  was measured and output to the electro-hydraulic shaker controller via measurement and control equipment. This pathway introduced the considerable delay (ca.  $6 \cdot 10^{-3}$  s) into front displacement excitation signal  $w_f$ , in comparison to  $w_r$ . The problem was solved by introduction of additional delay equal to:  $(T_{ex} - 6 \cdot 10^{-3})$  s into  $w_f$  pathway (where  $T_{ex}$  is the excitation period,  $T_{ex} = 1/f$ ) – the electro-hydraulic shaker duplicated the signal  $w_r$  with exactly one period delay.

## 4.2. Results and discussion

At the initial stage of the measurements we determined frequency transmissibilities of the open-loop system with no current in MR dampers' coils (hereafter called OS1:  $i_f = i_r = i_s = 0.0$  A). Figures 5 and 6 present the displacement amplitude transmissibilities  $T_x$  and  $T_{x_s}$  in comparison with the data predicted numerically. Accuracy of the experimentally obtained frequency of the first mode of damped bounce vibration  $f_1 = 2.63$  Hz is compromised by measurement frequency resolution (ca. 0.25 Hz) and excitation inaccuracy. The second bounce mode and pitch mode of damped vibration were not obtained due to the excitations type (synchronous base excitations). However residual pitch was present due to the nonlinearity of MR dampers characteristics.

The predicted transmissibility  $T_x$  (Fig. 5) is close to the measured one, but the resonance peak obtained experimentally is higher, most probably due to the inconsistency of MR dampers parameters. The predicted transmissibility  $T_{x_s}$  also reveals MR dampers modeling problems. The maximum amplitude of seat bouncing is shifted to the higher frequencies (in comparison with  $f_1$ ) due to the system nonlinearities (Fig. 6).

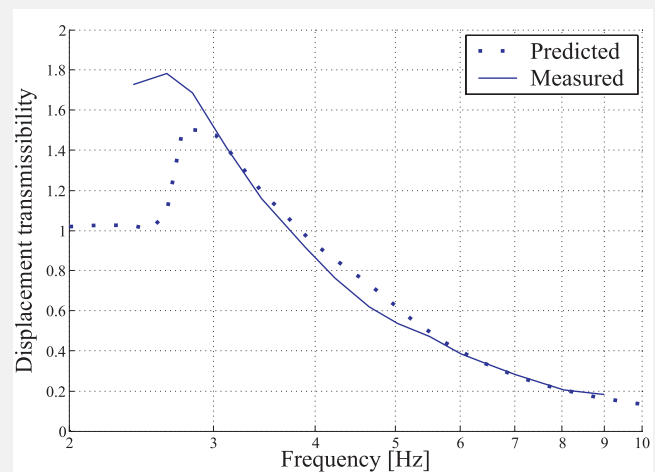


Fig. 5. Displacement transmissibility  $T_x$ : open-loop system OS1

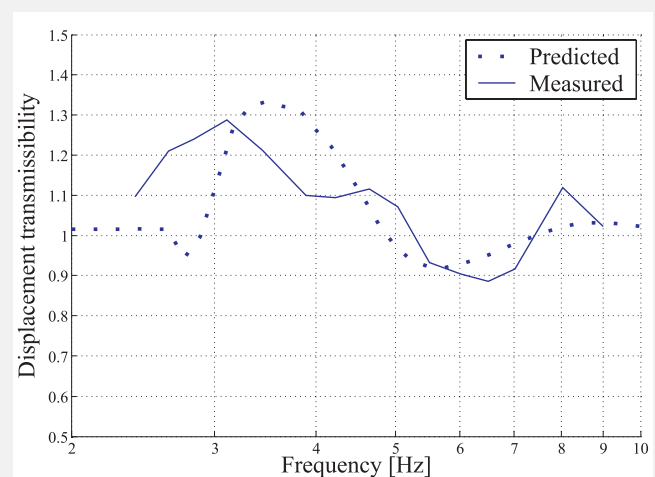


Fig. 6. Displacement transmissibility  $T_{x_s}$ : open-loop system OS1



In Figures 7, 9 and 11 we present RMS bounce acceleration transmissibilities of different feedback systems utilising: standard SH controller, SH with IM cascade controller, LQ with IM cascade controller. Figures 8, 10 and 12 show RMS bounce acceleration transmissibilities of open-loop system at 0.0 A (OS1) and at 0.2 A (OS2), and feedback system with LQ IM cascade controller.

When considering transmissibility indexes  $T_x$  and  $T_{x_s}$ , and the most essential one regarding drive comfort – the cumulative transmissibility  $T_C$ , the cascade controller LQ IM provides generally the best vibroisolation properties within the frequency range of (2.5, 10) Hz (comprising the most harmful for human spectrum), in comparison mainly with OS1, and other feedback systems. Standard SH feedback system transmissibilities reveal – resonance vibration reduction (in comparison with OS1), however they exhibit its poor (close to OS2) behaviour at higher frequencies. An interesting alternative is SH IM feedback system which omits this bark, but suffers of insufficient damping in resonance neighborhood.

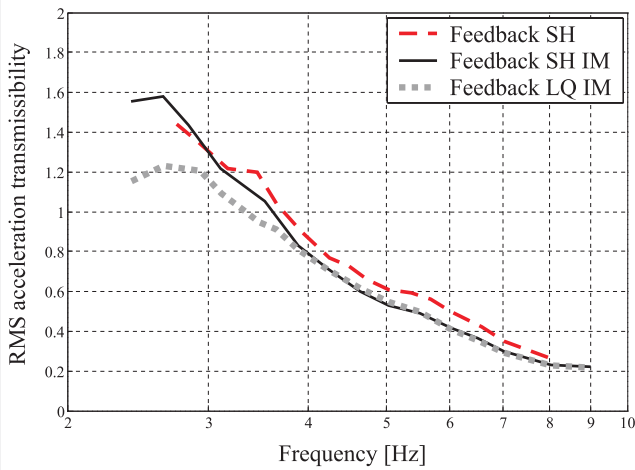


Fig. 7. RMS transmissibility  $T_x$ : feedback systems comparison

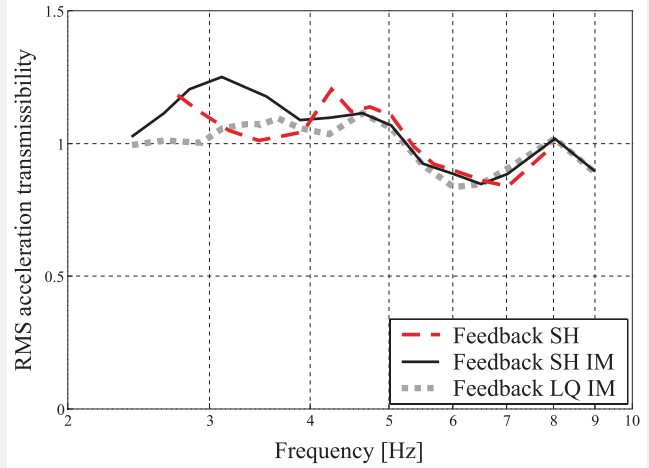


Fig. 9. RMS transmissibility  $T_{x_s}$ : feedback systems comparison

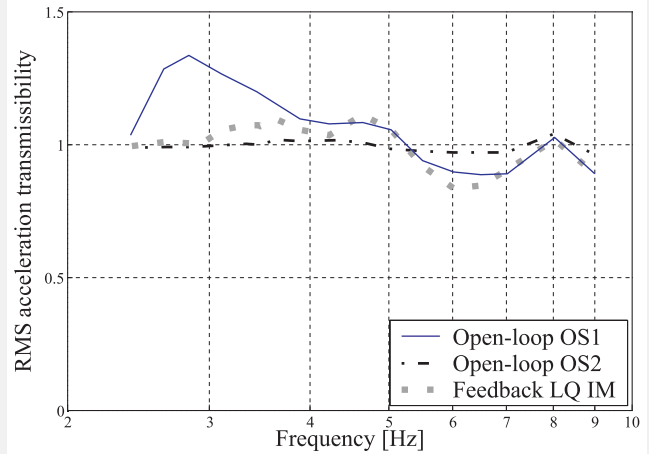


Fig. 10. RMS transmissibility  $T_{x_s}$ : open-loop and feedback systems comparison

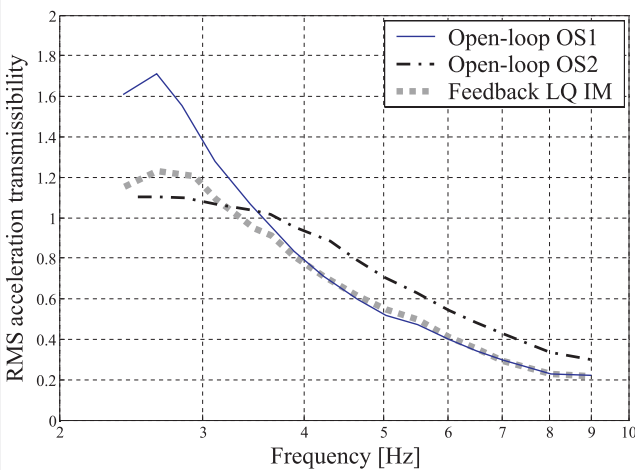


Fig. 8. RMS transmissibility  $T_x$ : open-loop and feedback systems comparison

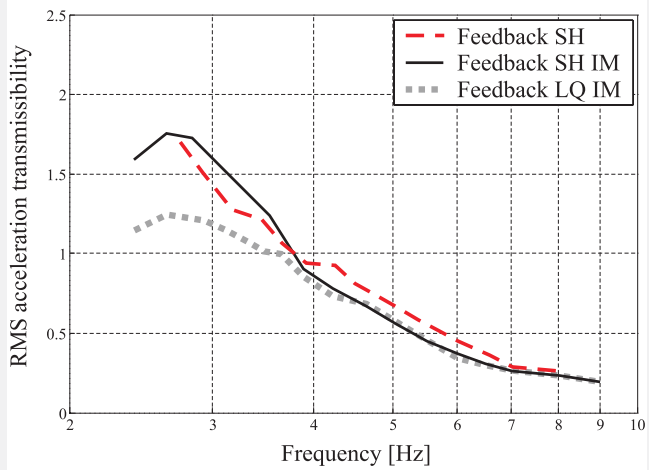
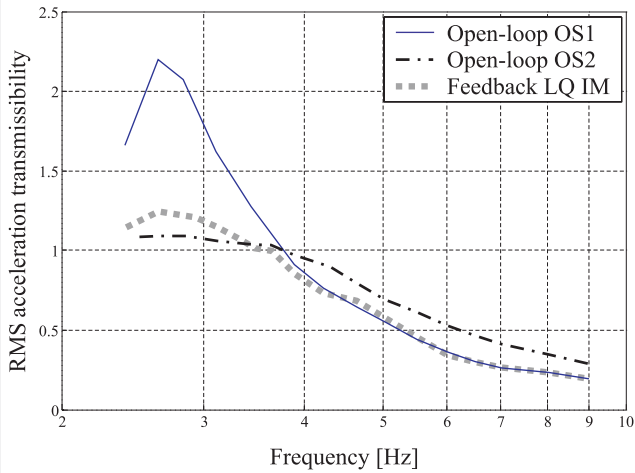
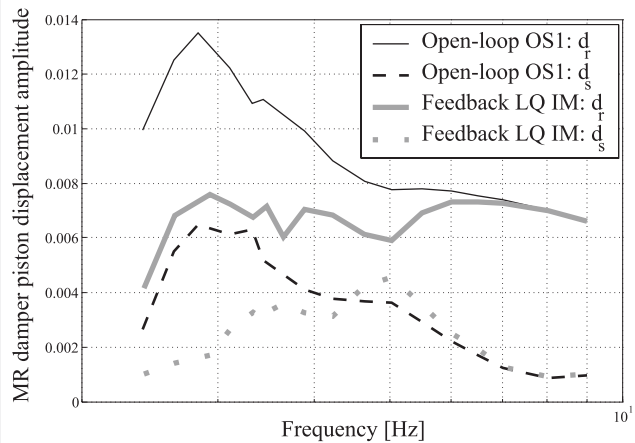


Fig. 11. RMS transmissibility  $T_C$ : feedback systems comparison



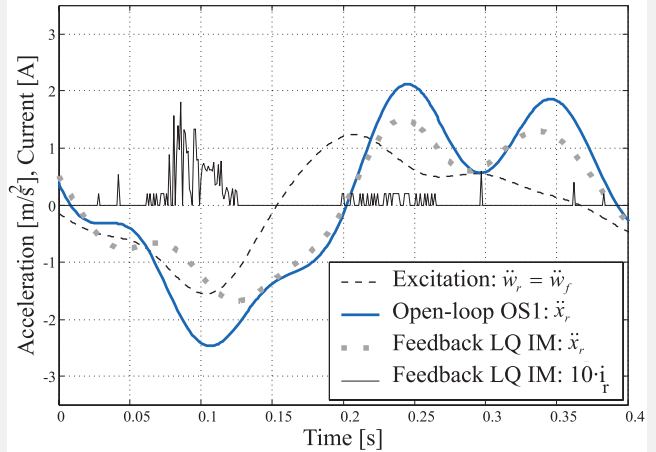
**Fig. 12.** RMS transmissibility  $T_C$ : open-loop and feedback systems comparison

Figure 13 shows dampers  $d_r$  and  $d_s$  piston displacement amplitude (peak to peak) vs. excitation frequency for OS1 and LQ IM systems. The previous experiments evidence that RD-1005-3 transmissibility depends on its piston displacement amplitude (the strongest dependence was observed for OS1). For the piston displacement amplitude values significantly below commonly set in our research  $7.5 \cdot 10^{-3}$  m, MR damper equivalent stiffness and damping factors both increase (thus resistance force also increases), resulting in higher transmissibility above resonance zone. This condition affects transmissibilities:  $T_{x_s}$  (Fig. 6) and  $T_{\dot{x}_s}$  (Fig. 9 and 10) above 6 Hz, where their rising, instead of falling can be observed.



**Fig. 13.** Piston displacement amplitude vs excitation frequency

Time patterns of accelerations:  $\ddot{x}_r$ ,  $\ddot{w}_r$ ,  $\ddot{x}_s$ ,  $\ddot{x} + \ddot{x}_s$  and currents:  $i_r$ ,  $i_s$  for synchronous semi-sine excitations  $w_f = w_r$  of dominant frequency  $f = 2.63$  Hz (at first mode of damped bounce vibration) for OS1 (open-loop) and LQ IM (feedback) systems are shown in Figures 14 and 15. Time patterns of:  $\ddot{x}_r$ ,  $\ddot{w}_r$ ,  $\ddot{x}_s$ ,  $\ddot{x} + \ddot{x}_s$ ,  $i_r$ ,  $i_s$  for synchronous semi-sine excitations  $w_f = w_r$  of dominant frequency  $f = 3.33$  Hz for OS1 and LQ IM systems are presented in Figures 16 and 17.



**Fig. 14.** Time response at 2.63 Hz

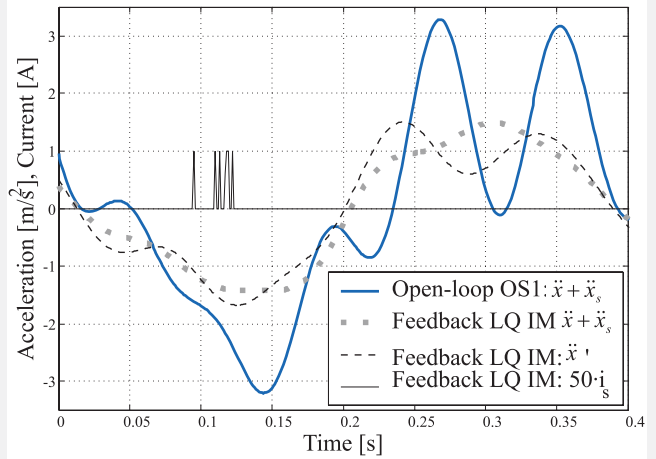


**Fig. 15.** Time response at 2.63 Hz

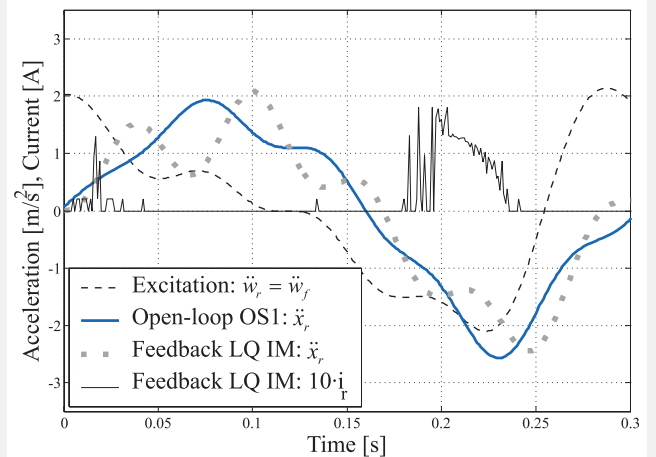


**Fig. 16.** Time response at 3.33 Hz

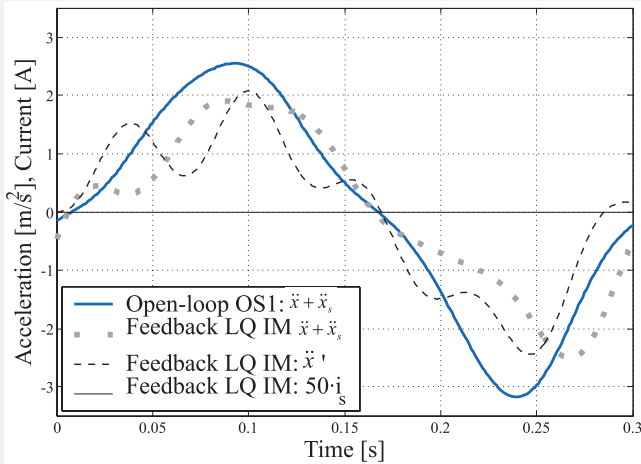


Fig. 17. Time response at 3.33 Hz

Figures 14–17 show the controller operation: current is set, when damper's  $d_r$  or  $d_s$  base acceleration (dashed black line:  $\ddot{w}_r$  or  $\ddot{x}$  respectively) derivative changes sign earlier than acceleration (dotted grey line:  $\ddot{x}_r$  or  $\ddot{x} + \ddot{x}_s$ , respectively) derivative of the mass suspended by the respective damper, thus leads to accelerations minimisation.

It can be observed that value of current  $i_s$  is constantly zero for LQ IM system at 3.33 Hz (Fig. 17), while seat absolute acceleration ( $\ddot{x} + \ddot{x}_s$ ) reduction in comparison with OS1 occurs. The reduced amplitude of  $d_s$  piston displacement (Fig. 13) for LQ IM system (in comparison with OS1) due to beam control via currents  $i_f$  and  $i_r$  (Fig. 16) results in  $d_s$  equivalent stiffness and damping factors increase (thus no increase of  $i_s$  is necessary).

Results listed in Table 1 are borne out by the values of frequency weighted RMS bounce acceleration transmissibility indexes  $V_{\ddot{x}}$  (2.15),  $V_{\ddot{x}_s}$  (2.16),  $V_C$  (2.17), derived in respect to [3]. It is worth to underline that values of all three weighted transmissibility indexes:  $V_{\ddot{x}}$ ,  $V_{\ddot{x}_s}$  and  $V_C$  for feedback system LQ IM are significantly lower than for both passive suspension systems OS1 and OS2, and for other feedback systems including standard skyhook (SH).

Table 1  
Frequency weighted RMS acceleration transmissibility

Open-loop system		
OS1	OS2	
$i_f = i_r = i_s = 0.0 \text{ A}$	$i_f = i_r = i_s = 0.2 \text{ A}$	
$V_{\ddot{x}} = 2.790 \cdot 10^3$	$V_{\ddot{x}} = 2.685 \cdot 10^3$	
$V_{\ddot{x}_s} = 3.794 \cdot 10^3$	$V_{\ddot{x}_s} = 3.615 \cdot 10^3$	
$V_C = 3.289 \cdot 10^3$	$V_C = 2.672 \cdot 10^3$	
Feedback system		
SH	SH IM	LQ IM
$V_{\ddot{x}} = 2.761 \cdot 10^3$	$V_{\ddot{x}} = 2.710 \cdot 10^3$	$V_{\ddot{x}} = 2.455 \cdot 10^3$
$V_{\ddot{x}_s} = 3.925 \cdot 10^3$	$V_{\ddot{x}_s} = 3.732 \cdot 10^3$	$V_{\ddot{x}_s} = 3.581 \cdot 10^3$
$V_C = 3.019 \cdot 10^3$	$V_C = 3.026 \cdot 10^3$	$V_C = 2.507 \cdot 10^3$

## 5. CONCLUSIONS

The developed quasi-optimal control strategy (LQ IM) proves to be the best choice for base vibration isolation in the resonance neighborhood and at higher frequencies. The obtained results encourage authors to further analysis and experiments, comprising modelling of MR damper behaviour, implementation of the LQ IM controller on the phyCORE-MPC555 embedded system, and possible redesign of the experimental setup. This work, supported by the research programme No. 4T07C 016 30, will solve questions present in the current paper, and will be the subject of further publications.

The paper presents the work done during the course of Smart Technology Expert School, operating in the Institute of Fundamental Technological Research (Warsaw, Poland).

## References

- [1] Ahmed A.K.W.: *Encyclopedia of Vibration*. Academic Press 2002
- [2] De Man P., Lemerle P., Mistrot P., Verschueren J-Ph., Preumont A.: *An investigation of a semi-active suspension for a fork lift truck*. Vehicle System Dynamics, vol. 43, No. 2, 2005
- [3] ISO Standard 2631-1: Mechanical vibration and shock – Evaluation of human exposure to whole-body vibration. 1997
- [4] Karnopp D., Crosby M.J., Harwood R.A. 1974: *Vibration Control Using Semi-Active Force Generators*. Journal of Engineering for Industry, 1974, pp. 619–626
- [5] Kashani R., Strelow J.E.: *Fuzzy Logic Active and Semi-Active Control of Off-Road Vehicle Suspension*. Vehicle System Dynamics, vol. 32, No. 4–5, 1999
- [6] Lai C.Y., Liao W.H.: *Vibration Control of a Suspension System via a Magnetorheological Fluid Damper*. Journal of Vibration and Control, No. 8, 2002
- [7] Marro G., Ntogramatzidis L.: *A contribution to the finite-horizon LQ control*. Incontro in ricordo di Giovanni Zappa, Florencja, Wlochy, 2005
- [8] Martynowicz P.: *Synteza algorytmów sterowania drganiami dla płaskiego modelu magnetoreologicznego zawieszenia pojazdu*. AGH UST 2006 (PhD Thesis)
- [9] Martynowicz P., Sapiński B.: *Pitch-plane Models of MR Vehicle Suspension for Experimental Testing*. Quarterly Mechanics, AGH UST Press, 24, 2005, pp. 120–123
- [10] Michałowski S.: *Wielofunkcyjne układy sterowania drgań pojazdów i maszyn roboczych*. IV Szkoła Metody Aktywne Redukcji Drgan i Hałasu, 1999, 189–196
- [11] Murata Y., Maemori K.: *Optimum Desing of ER Dampers for Ambulances*. JSME International Journal, Series C, vol. 42, No. 4, 1999
- [12] Nagai M.: *Semi-active control of vehicle vibration using continuously variable damper*. 3rd Int. Conf. on Motion and Vibration Control, Chiba, China 1996, pp. 153–159
- [13] Queslati F., Sankar S.: *A class of semi-active suspension schemes for vehicle vibration control*. Journal of Sound and Vibration, vol. 172, No. 3, 1994, pp. 391–411
- [14] Pare C.A., Ahmadian M.: *Experimental Evaluation of Semiactive Magneto-Rheological Dampers for Passenger Vehicles*. Proceedings of the 32nd International Symposium on Automotive Technology and Automation (ISATA), Vienna, Austria 1999
- [15] Sapiński B., Martynowicz P.: *Experimental Study of Vibration Control in a Two-Degree-of-Freedom Pitch-Plane Model of a Magnetorheological Vehicle Suspension*. Quarterly Mechanics, AGH UST Press, 26, 2007, pp. 60–70
- [16] Vavreck A.N.: *Control of a Dynamic Vibration Absorber with Magneto-rheological Damping*. Proceedings of SPIE, 4073, 2000, 252–263

- [17] Yasuda E., Doi S., Hattori K., Suzuki H., Hayashi Y.: *Improvement of Vehicle Motion and Riding – Comfort by Active Controlled Suspension System*. A Transaction of American Society of Automotive Engineers, 1991, No. 910662
- [18] Yokoyama M., Hedrick J.K., Toyama S.: *A Model Following Sliding Mode Controller for Semi-Active Suspension Systems with MR Dampers*. Proceedings of the American Control Conference, Arlington, USA 2001
- [19] Zhaoxiang D., Zifan F., Zhigang Z., Ming Z.: *Research on Virtual Prototyping System for Ground Vehicle with Magnetorheological Semi-active Suspension*. Proc. of the Symposium on Smart Materials for Engineering and Biomedical Applications, Suzhou, China, China Aviation Industry Press 2004
- [20] Zribi M., Karkoub M.: *Robust control of a car suspension system using magnetorheological dampers*. Journal of Vibration and Control, vol. 10, 2004, pp. 507–524